The Relationship between Seismicity and Fault Structure on the Discovery Transform Fault, East Pacific Rise

Monica Wolfson-Schwehr,[1] Margaret S. Boettcher,[1] Jeffrey J. McGuire,[2] and John A. Collins[2]

1. Generation of the Microseismic Earthquake Catalog

The catalog of microseismicity was generated using STA/LTA-based detection algorithms [*Houliston et al.*, 1984] for P-waves and wavelet-based detections [*Simons et al.*, 2006] for S-wave arrivals. Associations were based on both P- and S-wave arrivals, and required a minimum of 5 phases. P-wave arrivals were picked from waveforms that were bandpass filtered between 8 - 18 Hz, with time windows of 0.5 s for short-term average and 2.0 s for the long-term average, and a signal-to-noise ratio of 2.5. S-wave arrivals were picked from waveforms bandpass filtered between 1 - 10 Hz and windowed into a 5.12 s long time-series starting at the time of the P-wave pick. These waveforms were then decomposed into their wavelet coefficients using the Cohen-Daubechies-Feauveau wavelet basis. Picks were calculated as the first coefficient of the second scale to exceed a threshold as discussed in *Simons et al.* [2006]. Maximum travel time residuals were set to 1.0 s and 1.5 s for P-waves and S-waves, respectively. Over 24,000 microseismic events were

Corresponding author: M. Wolfson-Schwehr, Department of Earth Sciences, University of New Hampshire, Durham, NH 03824, USA. (monica.schwehr@gmail.com)

detected on Discovery during the deployment period, consequently an analyst did not go through and review all the picks.

2. Extension of Microseismicity beyond the Active Fault Trace

The extension of microseismicity beyond the active fault trace is observed at both the western RTI and the transform-ITSC intersection. Similar behavior is not observed along the neighboring Gofar transform fault. These regions of extension are located outside the OBS array, suggesting that the event locations may be the result of poor location estimates in both the STA/LTA and HypoDD-relocated catalogs. In order to investigate this we compare the S-wave and P-wave arrivals for two earthquakes, one located outside the western RTI and one located on the western fault segment, at three OBS stations along Discovery.

All three stations used in this comparison are broadband accelerometers with strong motion detectors. Stations D02 and D03 are located ∼6 km from the RTI and are situated on either side of the fault. Station D01 is located ∼11 km from the RTI, directly on the fault. Event 1, mL 3.2, is located ∼4 km west of the RTI and event 2, mL 3.1, is located ∼3 km east of the RTI, directly on the fault. For both events, the P-waves and S-waves arrive at stations D03 and D02 first, and then station D01, as expected. The arrival times for event 1 are longer relative to event 2 at all three stations, suggesting that it is, indeed, located west of event 1 and the RTI (Fig. S1).

3. Possible Explanations for the Existence of the Microseismic Gap

Three possible explanations for the existence of the gap in microseismicity seen in the relocated event positions have been considered. The preferred explanation is that the

gap is real, and reflects an area of the fault that was completely locked during 2008. *McGuire and Collins* [2013] used seafloor geodesy to show that this part of the fault was locked during 2008, and this is the explanation discussed in the main text. The other two explanations involve measurement errors. The exact velocity structure underlying the seismic gap on Discovery is not known; however, it is possible that an extreme low velocity anomaly exists in this region. However, by analogy to Gofar [*Roland et al.*, 2012; *Froment et al.*, 2014], this area is expected to have a relatively fast velocity structure as it coincides with the location of the largest repeating-rupture patch. Furthermore, the 1D velocity model used in HypoDD to relocate the microseismic events on Discovery already accounts for significantly reduced velocities in the crust (reductions up to 0.5 - 1.0 km/s, ∼10 - 20%) based on the results of a tomographic inversion of the P-wave velocity structure on Gofar [*Roland et al.*, 2012]. It seems unlikely, therefore, that there is a localized zone around station D01 in which seismic velocities are reduced even further. A third possibility is that a clock bias at station D01 is responsible for creating the gap. If arrivals at station D01 were recorded at a later time than they actually arrived, the event locations would be pushed away from the station. However, a clock bias would be accommodated to some degree by the HypoDD relocation process, and would be evident as relatively high time residuals for events pairs involving events recorded at station D01. The fact that relatively high time residuals are not seen in the data, combined with the seemingly low likelihood of a significant low velocity zone underlying station D01 and no movement in the geodetic data, suggests that the gap in microseismicity is a real feature.

References

Froment, B., P. Gouédard, E. C. Roland, H. Zhang, J. A. Collins, R. D. van der Hilst, and J. J. McGuire (2014), Imaging along-strike variations in mechanical properties of the Gofar transform fault, East Pacific Rise, *J. Geophys. Res.*, doi:10.1002/2014JB011270, in press.

Houliston, D. J., G. Waugh, and J. Laughlin (1984), Automatic real-time event detection for seismic networks, *Comput. Geosci.*, *10*(4), 431–436, doi:10.1016/0098-3004(84)90043-8.

McGuire, J. J., and J. A. Collins (2013), Millimeter-level precision in a seafloor geodesy experiment at the Discovery transform fault, East Pacific Rise, *Geochem. Geophys. Geosys.*, *14*(1), 4392–4402, doi:10.1002/ggge.20225.

Roland, E. C., D. Lizarralde, J. J. McGuire, and J. A. Collins (2012), Seismic velocity constraints on the material properties that control earthquake behavior at the Quebrada-Discovery-Gofar transform faults, East Pacific Rise, *J. Geophys. Res.*, *117*(B11102), doi:10.1029/2012JB009422.

Simons, F. J., B. D. E. Dando, and R. M. Allen (2006), Automatic detection and rapid determination of earthquake magnitude by wavelet multiscale analysis of the primary arrival, *Earth Planet. Sci. Lett.*, *250*(1-2), 214–223, doi:10.1016/j.epsl.2006.07.039.

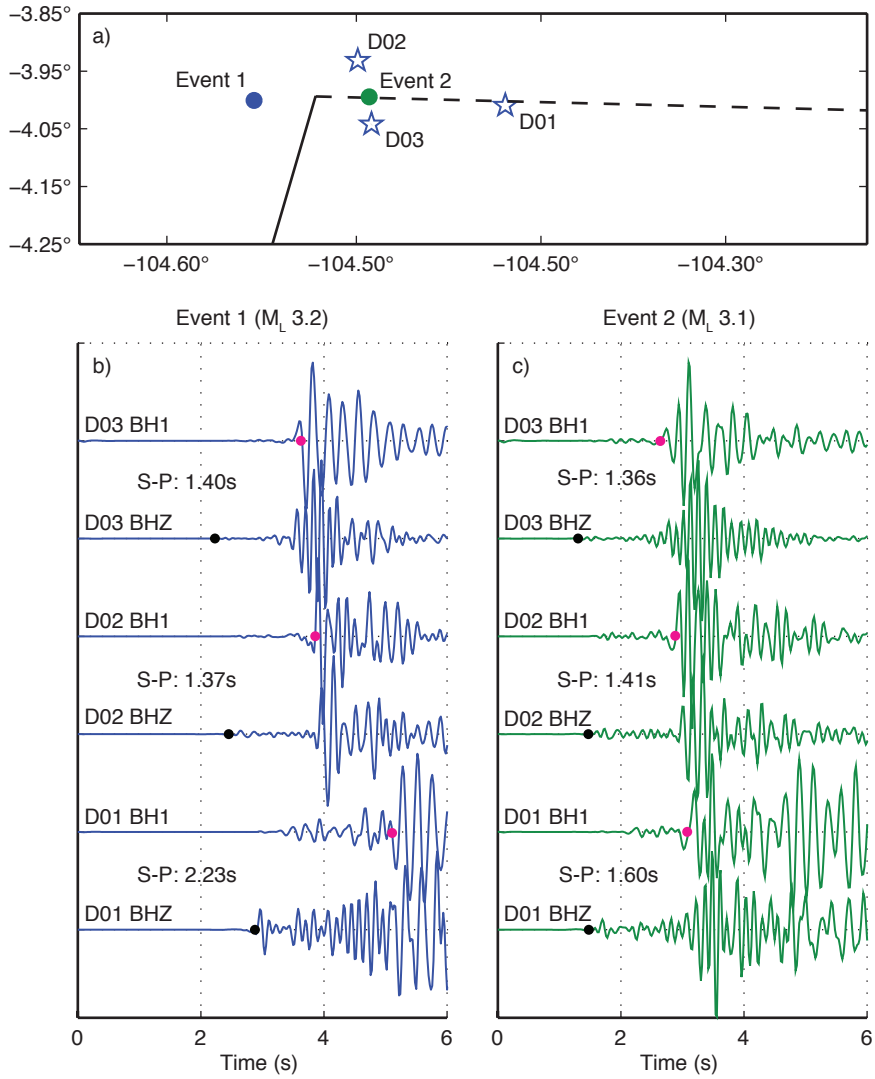

Figure S1. (a) Simplified map-view of DW. The dashed-line represents the active transform fault and the solid line denotes the EPR. Blue stars denote the location of stations D01 - D03. Event 1 (blue circle) is located ∼4 km west of the RTI. Event 2 (green circle) is located ∼3 east of the RTI. Both events are shown at their relocated positions. (b) and (c) show the waveform arrivals at stations D01, D02, and D03 for event 1 and event 2, respectively. BH1 is one of the horizontal components of the seismometer and BHZ is the vertical. Waveforms are bandpass filtered between 2 and 10 Hz. The black dots on the BHZ waveforms mark the P-wave arrival, while the pink dots on the BH1 waveforms mark the S-wave arrival.